OPEN ACCESS Freely available online

PLOS ONE

Glycogen Phosphorylase Inhibitor N-(3,5-Dimethyl-Benzoyl)-N′-(β-D-Glucopyranosyl)Urea Improves Glucose Tolerance under Normoglycemic and Diabetic Conditions and Rearranges Hepatic Metabolism

Lilla Nagy[1☯], Tibor Docsa[1☯], Magdolna Szántó[1,2], Attila Brunyánszki[1], Csaba Hegedűs[1], Judit Márton[1], Bálint Kónya[3], László Virág[1,2], László Somsák[3], Pál Gergely[1,2], Péter Bai[1,2]*

1 Department of Medical Chemistry, University of Debrecen Medical and Health Science Center, Debrecen, Hungary, **2** Cell Biology and Signaling Research Group of the Hungarian Academy of Sciences, Debrecen, Hungary, **3** Department of Organic Chemistry, University of Debrecen, Debrecen, Hungary

Abstract

Glycogen phosphorylase (GP) catalyzes the breakdown of glycogen and largely contributes to hepatic glucose production making GP inhibition an attractive target to modulate glucose levels in diabetes. Hereby we present the metabolic effects of a novel, potent, glucose-based GP inhibitor (KB228) tested *in vitro* and *in vivo* under normoglycemic and diabetic conditions. KB228 administration enhanced glucose sensitivity in chow-fed and obese, diabetic mice that was a result of higher hepatic glucose uptake. Besides improved glucose sensitivity, we have observed further unexpected metabolic rearrangements. KB228 administration increased oxygen consumption that was probably due to the overexpression of uncoupling protein-2 (UCP2) that was observed in animal and cellular models. Furthermore, KB228 treatment induced mammalian target of rapamycin complex 2 (mTORC2) in mice. Our data demonstrate that glucose based GP inhibitors are capable of reducing glucose levels in mice under normo and hyperglycemic conditions. Moreover, these GP inhibitors induce accommodation in addition to GP inhibition - such as enhanced mitochondrial oxidation and mTORC2 signaling – to cope with the glucose influx and increased glycogen deposition in the cells, however the molecular mechanism of accommodation is unexplored.

Citation: Nagy L, Docsa T, Szántó M, Brunyánszki A, Hegedűs C, et al. (2013) Glycogen Phosphorylase Inhibitor N-(3,5-Dimethyl-Benzoyl)-N′-(β-D-Glucopyranosyl)Urea Improves Glucose Tolerance under Normoglycemic and Diabetic Conditions and Rearranges Hepatic Metabolism. PLoS ONE 8(7): e69420. doi:10.1371/journal.pone.0069420

Editor: Laszlo Buday, Hungarian Academy of Sciences, Hungary

Received April 16, 2013; **Accepted** June 10, 2013; **Published** July 25, 2013

Funding: This work was supported by grants from the National Innovation Office (Baross program Seahorse grant; TéT_09-2010-0023), OTKA CNK80709, CK77712, K82009, K75864, PD83473, TÁMOP 4.2.2/B-10/1-2010-0024, TÁMOP 4.2.1/B-09/1/KONV-2012-0025, TÁMOP-4.2.1./B-09/KONV-2010-0007 and Medical and Health Science Center (Mecenatura Mec-8/2011). PB, TD and MS were recipients of Bolyai fellowships of the Hungarian Academy of Sciences. The funders had no role in study design, data collection and analysis, decision to publish, or preparation of the manuscript.

Competing Interests: The authors have declared that no competing interests exist.

* E-mail: baip@med.unideb.hu

☯ These authors contributed equally to this work.

Introduction

Glycogen content of tissues and cells depend on the concerted regulation of glycogen synthesis by glycogen synthase (GS) and glycogen breakdown by glycogen phosphorylase (GP) through an intricate network of signal transduction pathways related to hormonal signaling [1]. These signal transduction pathways, converging on GS and GP, exert their regulatory activity through the posttranslational modification of these enzymes to meet the energy demands of the organism [2–4].

GP activity is crucial in fine tuning hepatic glycogen content and hepatic glucose homeostasis [5,6]. Glycogen breakdown by GP is associated with fasting responses that lead to enhanced hepatic glucose production (HGP) [7] that is reduced by GP inhibition. Moreover, GP inhibition enhances glycogen build-up in skeletal muscle and liver enhancing glucose uptake that contributes to glucose clearance from blood [8,9]. Inhibition of HGP and induction of glucose uptake together reduce blood glucose that makes GP a promising pharmaceutical target to manage serum glucose levels.

GP is a homodimeric enzyme existing in a phosphorylated (GPa) and an unphosphorylated form (GPb) [10]. Phosphorylase kinase phosphorylates GPb turning it to GPa, the active form [10]. Effectors influence GP activity by switching between the tense (T, less active) and relaxed (R, more active) states of both GPa and GPb. There are several effector binding sites on GP: the active site, the allosteric (AMP binding) site, the new allosteric (indole-carboxamide binding) site, the inhibitor (purin binding) site and the storage site. [11]. GP has three isoforms named after the tissues where it is dominantly expressed: liver (pygl), brain (pygb) and muscle (pygm). Most GP inhibitors (GPi-s) are unselective and inhibit all isoforms [10,11].

It is important to note that glucose is considered as a physiological regulator of GP [12]. However, glucose 6-phosphate exerts a similar effect on GP as glucose, although glucose and glucose 6-phosphate bind to different sites [13] and their binding

Table 1. Primers used in RT-qPCR reactions.

Gene		Forward primer	Reverse primer
β-actin	Human	5′-GACCCAGATCATGTTTGAGACC-3′	5′-CATCACGATGCCAGTGGTAC-3′
	Murine	5′-TGGAGAGCACCAAGACAGACA-3′	5′-TGCCGGAGTCGACAATGAT-3′
Cyclophylin	Human	5′-GTCTCCTTTGAGCTGTTTGCAGAC-3′	5′-CTTGCCACCAGTGCCATTATG-3′
	Murine	5′-CAAGGTCATCCATGACAACTTTG-3′	5′GGCCATCCACAGTCTTCTGG-3′
36B4	Human	5′-CCATTGAAATCCTGAGTGATGTG-3′	5′-GTCGAACACCTGCTGGATGAC-3′
	Murine	5′-AGATTCGGGATATGCTGTTGG-3′	5′-AAAGCCTGGAAGAAGGAGGTC-3′
UCP2	Human	5′-CTACAAGACCATTGCCCGGAG-3′	5′-ACAATGGCATTACGAGCAACA-3′
	Murine	5′-TGGCAGGTAGCACCACAGG-3′	5′-CATCTGGTCTTGCAGCAACTCT-3′
PYGL	Human	5′-GTGCCCCAAGAGGGTATATTAC-3′	5′-AAGAAGCAGGCAGCAAGTCTC-3′
	Murine	5′-CCCCGTGCCTGGATATATGA-3′	5′-TGTTTCAGCCGCAACTCCTT-3′
PYGM:	Human	5′-GGACCCCAAGAGGATCTACTACC-3′	5′-CCTCGTCACAGGCATTCTCTA-3′
	Murine	5′-CCCAAGAGGATCTACTACCTGTC-3′	5′-ACTCATAGCGGATCCCATAGC-3′
PYGB	Human	5′-AGCCATCTATCAGTTGGGGTTAG-3′	5′-TGCCAGCCATTGACAATCTTC-3′
	Murine	5′-CACTTATCAGTTGGGGTTGGAC-3′	5′-GCCAGTCATCAGCTTCTTCAAC-3′

doi:10.1371/journal.pone.0069420.t001

converts GPa to the T conformation making it more prone to dephosphorylation [13].

Research efforts have identified an ample number of structurally different, potent GPi-s (reviewed in [7,14]). Genetic or pharmacological inhibition of GP activity ameliorates glucose tolerance supporting the possible applicability of GP inhibition in the management of glucose handling disorders in diabetes [8,9,15–18]. Indeed, a GP inhibitor, CP-316819 (Ingliforib), in clinical study was able to reduce glucagon-induced hyperglycemia [11].

Our research group has been involved in the design of glucose-derived and other GPi-s [19,20]. In the current study we have characterized the metabolic effects of a novel glucose-based GPi N-(3,5-dimethyl-benzoyl)-N'-(β-D-glucopyranosyl)urea (**KB228**) in control, and diabetic mice and in cellular models.

Materials and Methods

Chemicals

Unless otherwise stated, all chemicals were from *Sigma-Aldrich* (St. Louis, MO, USA).

Glycogen phosphorylase inhibitors TH (D-glucopyranosylidene-spiro-thiohydantoin) [9], NV50 (*N*-(β-D-glucopyranosyl)-*N*'-(4-nitrobenzoyl) urea) [21] and NV76 (*N*-(β-D-glucopyranosyl)-*N*'-(2-naphthoyl) urea) [14,22] were synthesized in the laboratory of Dr. László Somsák and were described in the literature indicated.

Preparation of N-(3,5-dimethyl-benzoyl)-N′-(β-D-glucopyranosyl)urea

Preparation of acyl-isocyanates was adapted from literature [23]: Oxalylchloride (1.1 equivalent) was added to a suspension of 3,5-dimethyl-benzamide **2** [24] (200 mg, 1.341 mmol) in anhydrous 1,2-dichloroethane (15 mL) and the mixture was heated at reflux temperature for 1 day. The volatiles were distilled off under diminished pressure and toluene (2 × 5 mL) was evaporated from the residue to remove the rest of oxalylchloride. The crude acyl-isocyanate **3** obtained in this way was mixed with a solution of β-D-glucopyranosylammonium carbamate [25] (**1**, 320 mg, 1.341 mmol, 1 equivalent) in anhydrous pyridine (45 mL) and the mixture was stirred at room temperature for 4 days. Pyridine was distilled off under diminished pressure and evaporation of toluene (2 × 30 mL) removed traces of pyridine. The crude product was purified by silica gel column chromatography ($CHCl_3$-MeOH, 7:1) to give the target compound **4**.

Yield: 214 mg (45%), yellow syrup. $R_f = 0.21$ ($CHCl_3$-MeOH, 7:1) $[\alpha]_D$ +7.1 (c = 0.310, DMSO) ^{1}H NMR (DMSO-d_6, 360 MHz) δ (ppm) 10.70 (s, 1H, N*H*), 9.09 (d, 1H, J = 9.1 Hz, N*H*), 7.59 (s, 2H, Ar*H*), 7.26 (s, 1H, Ar*H*), 5.25 (d, 1H, J = 5.4 Hz, OH), 5.03 (d, 1H, J = 4.6 Hz, OH), 4.94 (d, 1H, J = 4.9 Hz, OH), 4.81 (t, 1H, J = 9.0, 9.0 Hz, H-1), 4.53 (pseudo t, 1H, J = 9.2, 8.9 Hz, OH), 3.65 (dd, 1H, J = 12.1, 2.3 Hz, H-6a), 3.42 (dd, 1H, J = 12.1, 3.9 Hz, H-6b), 3.25-3.00 (m, 4H, H-2, H-3, H-4, H-5), 2.32 (s, 6H, 2xCH_3).^{13}C NMR (DMSO-d_6, 90 MHz) δ (ppm) 169.2 (NH*C*OAr), 156.3 (NH*C*ONH), 133.9, 129.1, 126.7, 122.9

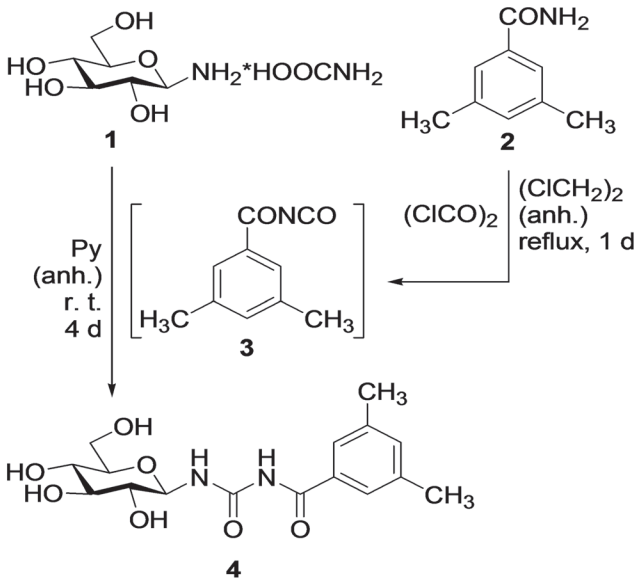

Figure 1. Synthesis of KB228. *N*-(3,5-dimethyl-benzoyl)-*N*'-(β-D-glucopyranosyl)urea (KB228), a GP inhibitor was prepared as described in the Materials and Methods section.
doi:10.1371/journal.pone.0069420.g001

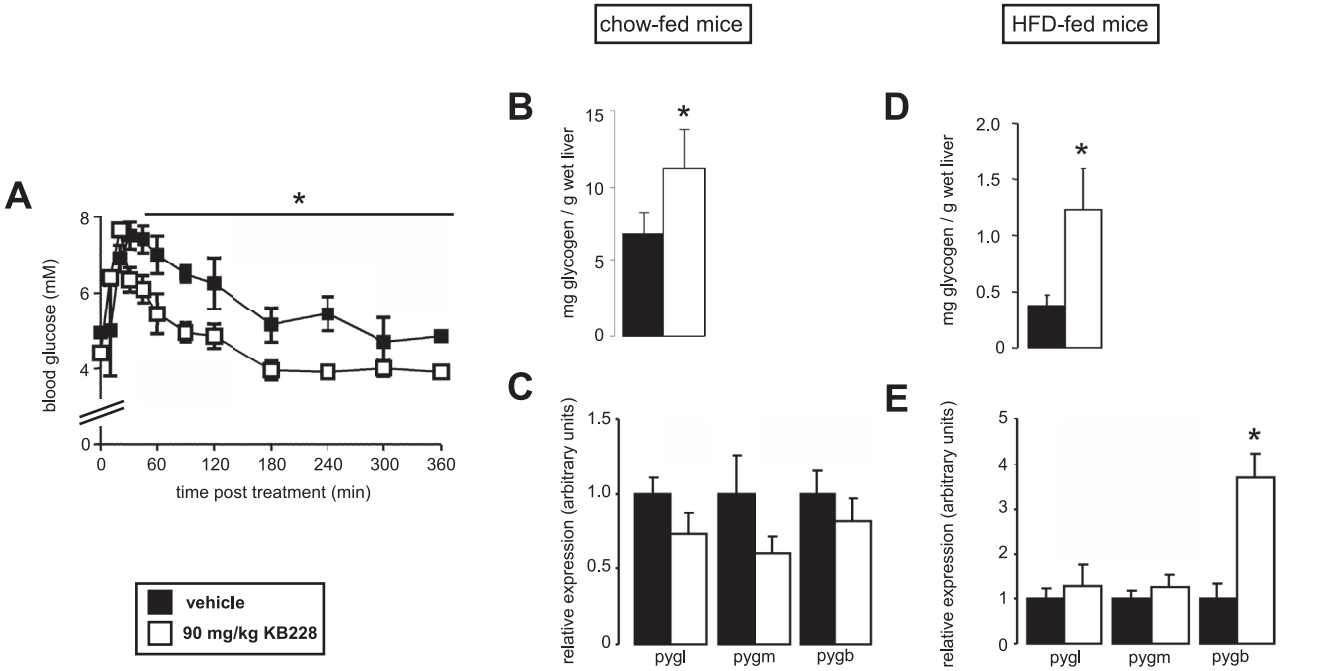

Figure 2. Characterization of the *in vivo* applicability of KB228. (A) C57/Bl6J male mice (n = 3/3, 3 months of age) were administered KB228, or vehicle (physiological saline, 1% DMSO) i.p., then blood glucose levels were determined using an Accu-Check glucometer (*Roche*). (B-C) Chow-fed C57/Bl6J male mice (n = 7/7, 6 months of age) were sacrificed 2 hours post treatment with KB228 (90 mg/kg) then (B) glycogen content and (C) the expression the liver, brain and muscle isoforms of GP (*pygl*, *pygb* and *pygm*, respectively) were determined using RT-qPCR. (D-E) HFD-fed C57/Bl6J male mice (n = 9/9, 6 months of age) were sacrificed 2 hours post treatment with KB228 (90 mg/kg) then (D) glycogen content and (E) the expression of the indicated genes were measured by RT-qPCR. * indicate statistically significant difference between vehicle and KB228-treated groups at $p<0.05$.
doi:10.1371/journal.pone.0069420.g002

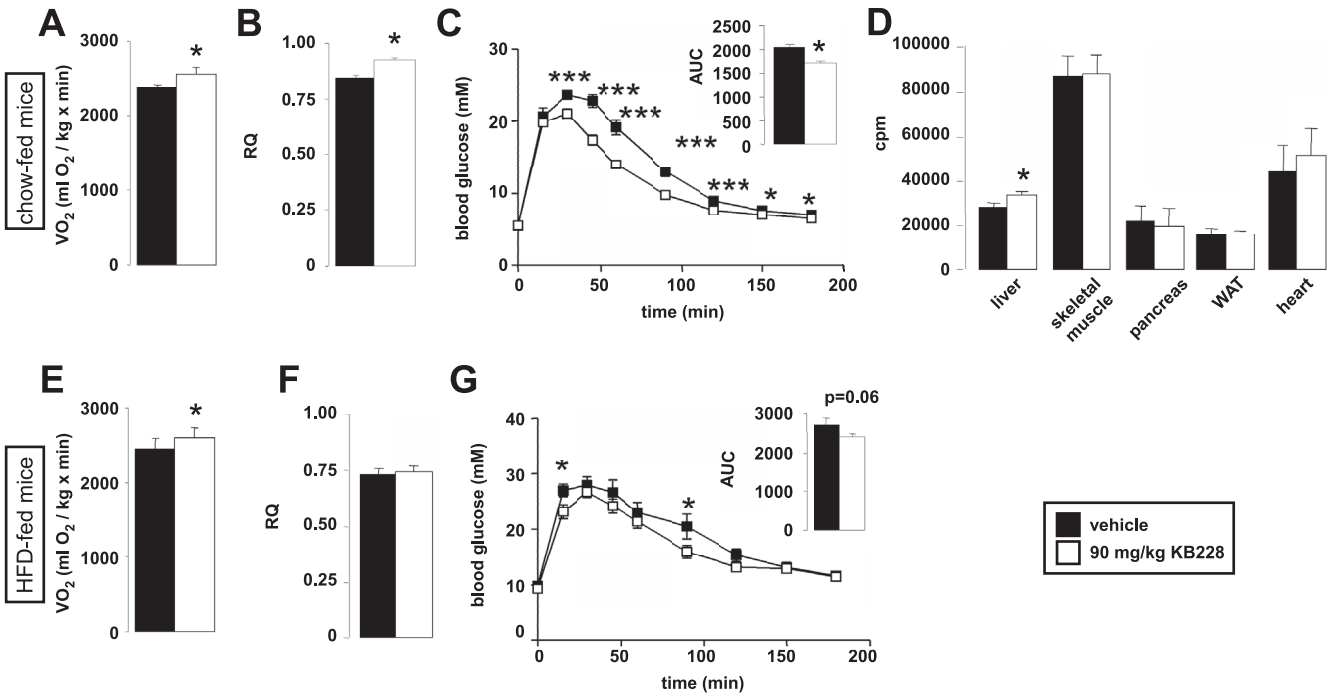

Figure 3. The impact of KB228 on *in vivo* glucose metabolism. (A-B) Chow-fed C57/Bl6J male mice (n = 7/7, 6 months of age) underwent vehicle or KB228 treatment, then (A) oxygen consumption and (B) RQ were determined in indirect calorimetry chambers. (C) The same cohorts of mice were subjected to an ipGTT test. (D) Chow-fed C57/Bl6J male mice (n = 4/4, 6 months of age) were subjected to a glucose uptake experiment as described in Materials and Methods. (E-F) HFD-fed C57/Bl6J male mice (n = 9/9, 6 months of age) underwent vehicle, or KB228 treatment, then (E) oxygen consumption and (F) RQ were determined in indirect calorimetry chambers. (G) The same cohorts of mice were subjected to an ipGTT test. * and *** indicate statistically significant difference between vehicle and KB228-treated groups at $p<0.05$, or $p<0.001$, respectively.
doi:10.1371/journal.pone.0069420.g003

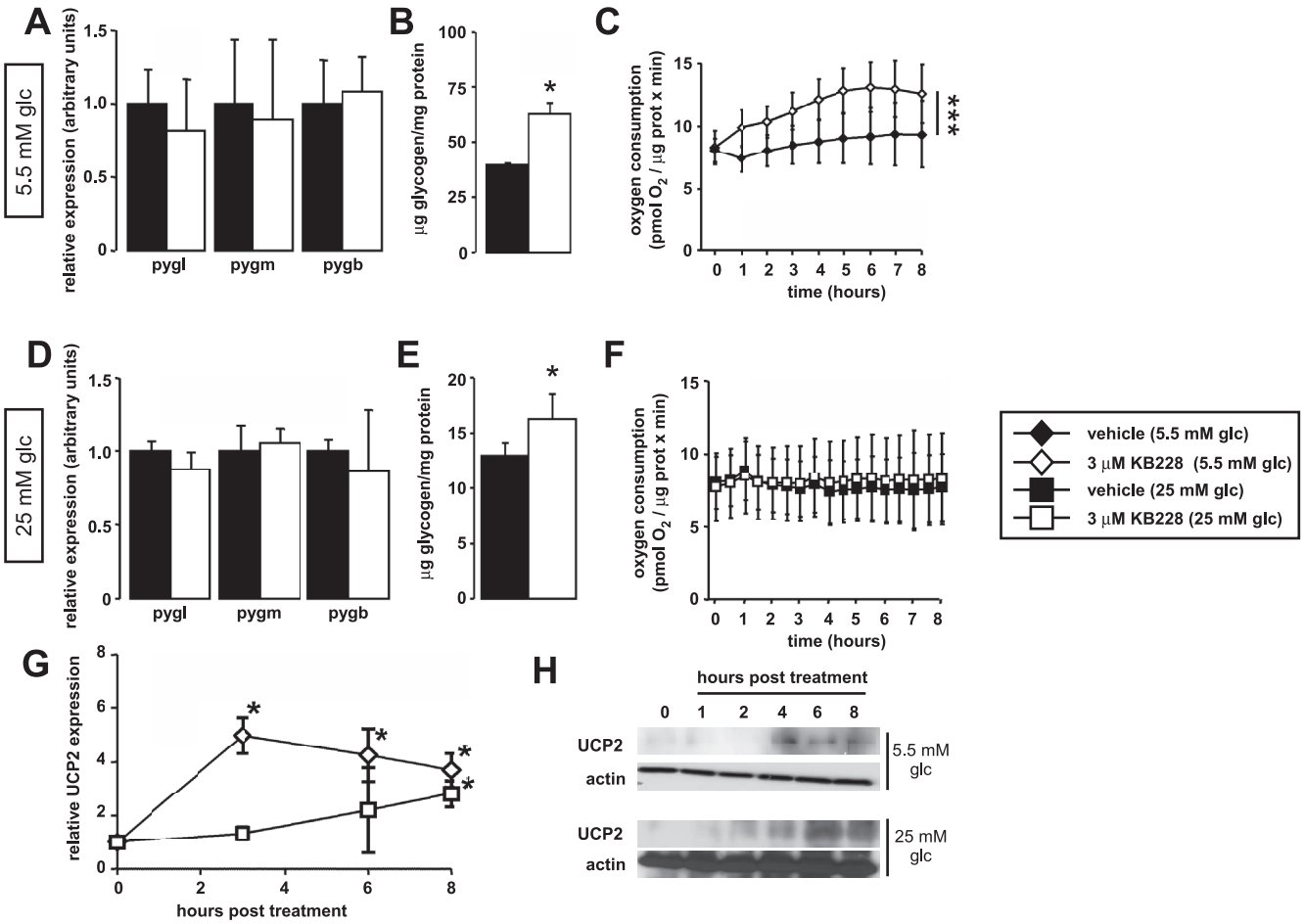

Figure 4. Metabolic effects of KB228 treatment in HepG2 cells. (A–C) In vehicle or KB228-treated HepG2 cells (n = 3/3) under normoglycemic conditions (A) the expression of GP isoforms, (B) glycogen content and (C) cellular oxygen consumption (OCR) were determined (n = 47/47). (D–F) In vehicle or KB228-treated HepG2 cells (n = 3/3) under hyperglycemic conditions (D) the expression of GP isoforms, (E) glycogen content and (F) cellular oxygen consumption (OCR) were determined (n = 47/47). (G–H) In vehicle, or KB228-treated HepG2 cells (n = 4/4) under normoglycemic and hyperglycemic conditions UCP2 (G) mRNA and (H) protein levels were determined by RT-qPCR and Western blotting, respectively. Error is given as SD throughout the figure. * and *** indicate statistically significant difference between vehicle and KB228-treated groups at $p<0.05$, or $p<0.001$, respectively.
doi:10.1371/journal.pone.0069420.g004

(Ar), 82.1 (C-1), 78.9, 78.1, 75.1, 71.7 (C-2–C-5), 63.0 (C-6), 22.3 (CH_3). Anal. Calcd for $C_{16}H_{22}N_2O_7$ (354.36): C, 54.23; H, 6.26; N, 7.91; Found: C, 54.37; H, 6.15; N, 8.03.

Biochemical Measurements

GP kinetic studies were performed as described in [26]. Determination of glycogen was as in [9].

Animal Studies

All animal experiments were carried out according to the national, EU and NIH ethical guidelines and were authorized by the Institutional Animal Care and Use Committee at the University of Debrecen (7/2010 DE MÁB). C57/Bl6J male mice (*Charles River*, Wilmington, MA, USA) had *ad libitum* access to water and chow (10 kcal% of fat) (SAFE, Augy, France) or hypercaloric high-fat diet (HFD, 60 kcal% of fat) (*Research Diets, Inc.*, New Brunswick, NJ, USA), and were kept in a 12 hr dark/light cycle (light 7 a.m. –7 p.m., night 7 p.m. –7 a.m.). All measurements took place 2 hours after injecting 90 mg/kg KB228 in a single intraperitoneal (i.p.) bolus unless otherwise stated. Intraperitoneal glucose tolerance test (ipGTT) and intraperitoneal insulin tolerance test (ipITT) was described in [27].

Indirect Calorimetry

Indirect calorimetry experiments were performed in a CLAMS system (*Columbus Instruments*, Columbus, OH, USA). Mice were habituated to the new environment of the cages for 24 hours. Then at 8 a.m. mice received a bolus i.p. injection of KB228 (90 mg/kg) or vehicle then were returned to the measurement cages and for the following six hours oxygen consumption and carbon dioxide release was recorded.

Glucose Uptake Experiments

In glucose uptake experiments mice were injected with 120 μCi/kg ^{14}C-2-deoxyglucose and 20 U/kg insulin through the jugular vein under halothane anaesthesia. The incision above the vein was closed with a suture. Blood glucose levels were monitored at the time of the suture, 15 and 30 minutes post intervention. Mice were sacrificed by cervical dislocation 30 minutes post intervention and the indicated organs were removed. Carefully weighed pieces of these tissues were solubilised in 0.5 ml

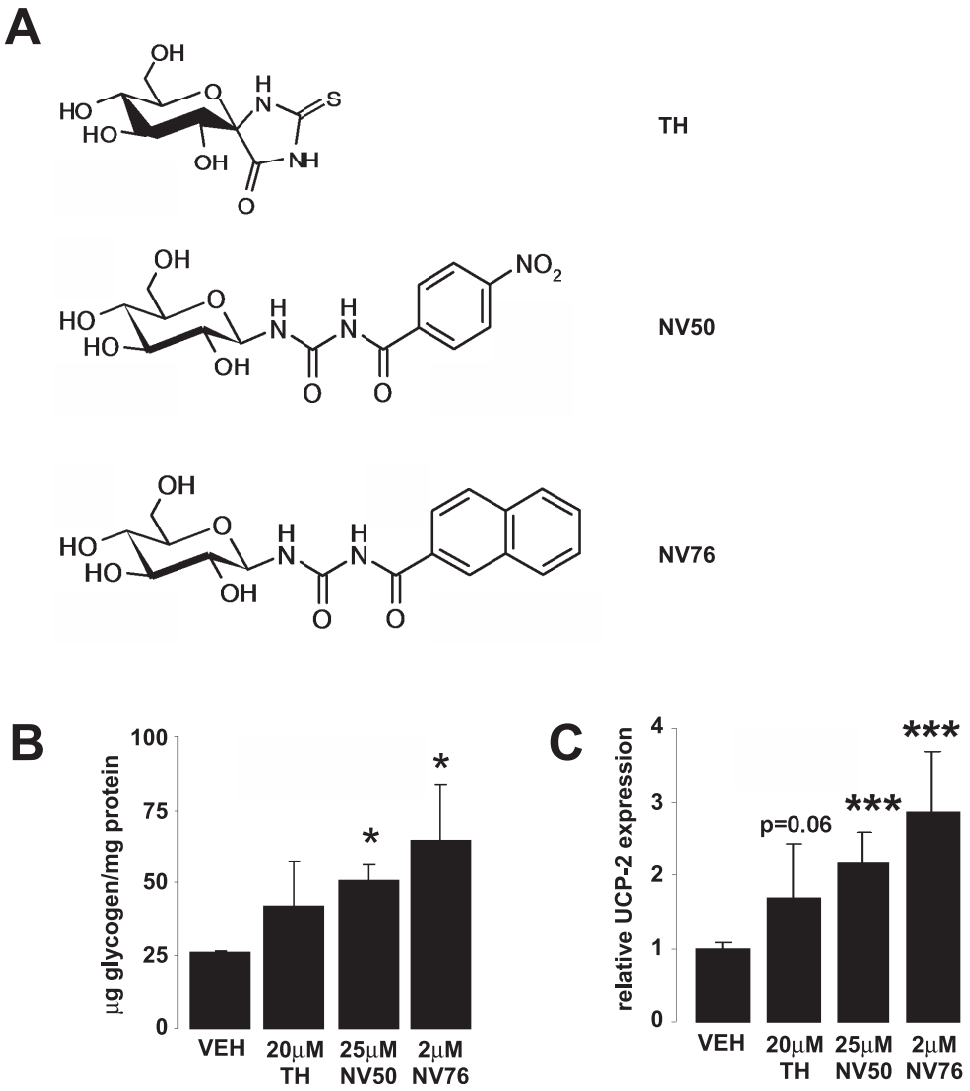

Figure 5. Other GPi-s also induce UCP2 expression in HepG2 cells. (A) Three GPi-s TH, NV50 and NV76 were tested on HepG2 cells. (B–C) HepG2 cells (n = 3) kept under normoglycemic conditions were treated with the inhibitors at the indicated concentrations for 8 hours, then (B) glycogen content and (C) UCP-2 expression was determined as described in Materials and Methods. Error is given as SD throughout the figure. * and *** indicate statistically significant difference between vehicle and GPi-treated groups at $p<0.05$, or $p<0.001$, respectively. VEH – vehicle, other abbreviations are in the text.
doi:10.1371/journal.pone.0069420.g005

1 M NaOH at 70°C for 60 minutes. Lysates were mixed with Aqualight HIBEX (*Personal Life Sciences*) scintillation liquid and were measured in a Wallac scintillation counter (*Perkin Elmer*, Waltham, MA, USA).

Cell Culture

HepG2 human hepatocarcinoma cells and C2C12 myoblasts were obtained from ATCC (Manassas, VA, USA) and were cultured in DMEM, 10% FCS, 1 g/L or 4.5 g/L glucose, as indicated. C2C12 cells were differentiated in DMEM, 2% horse serum 1 g/L glucose for 2 days as described in [27,28].

Cellular Oximetry

*O*xygen *c*onsumption *r*ate (OCR) of HepG2 cells were measured using an XF96 oxymeter (Seahorse Biosciences, North Billerica, MA, USA) similarly to [29]. Briefly, HepG2 cells were seeded in 96-well assay plates. After recording the baseline OCR cells received a single bolus dose of 3 μM KB228 or other GPi-s, as indicated. Then, OCR was recorded every hour to follow the effects of GPi-s. Final reading took place at 8 hours post-treatment. OCR was normalized to protein content and normalized readings were displayed.

cDNA Preparation, qPCR

Total RNA preparation, reverse transcription, and RT-qPCR were performed as in [30]. Expression was normalized to the geometric mean of three control genes (β-actin, cyclophylin, 36B4). Primers are summarized in Table 1.

Protein Extraction and Western Blotting

Western blotting experiments were performed as described in [28]. Blots were probed with the following antibodies: UCP2 (*Abcam*, Cambridge, UK, 1:1000), Akt-2 (*Cell Signalling*, Danvers, MA, USA, 1:1000), phospho-Akt-2 (^{473}Ser) (*Cell Signaling*, 1:2000), GSK3β (*Sigma-Aldrich*, 1:2000), phospho-GSK3β ($^{9/21}$Ser) (*Cell Signaling*, 1:1000) and actin (*Sigma-Aldrich*, 1:10000).

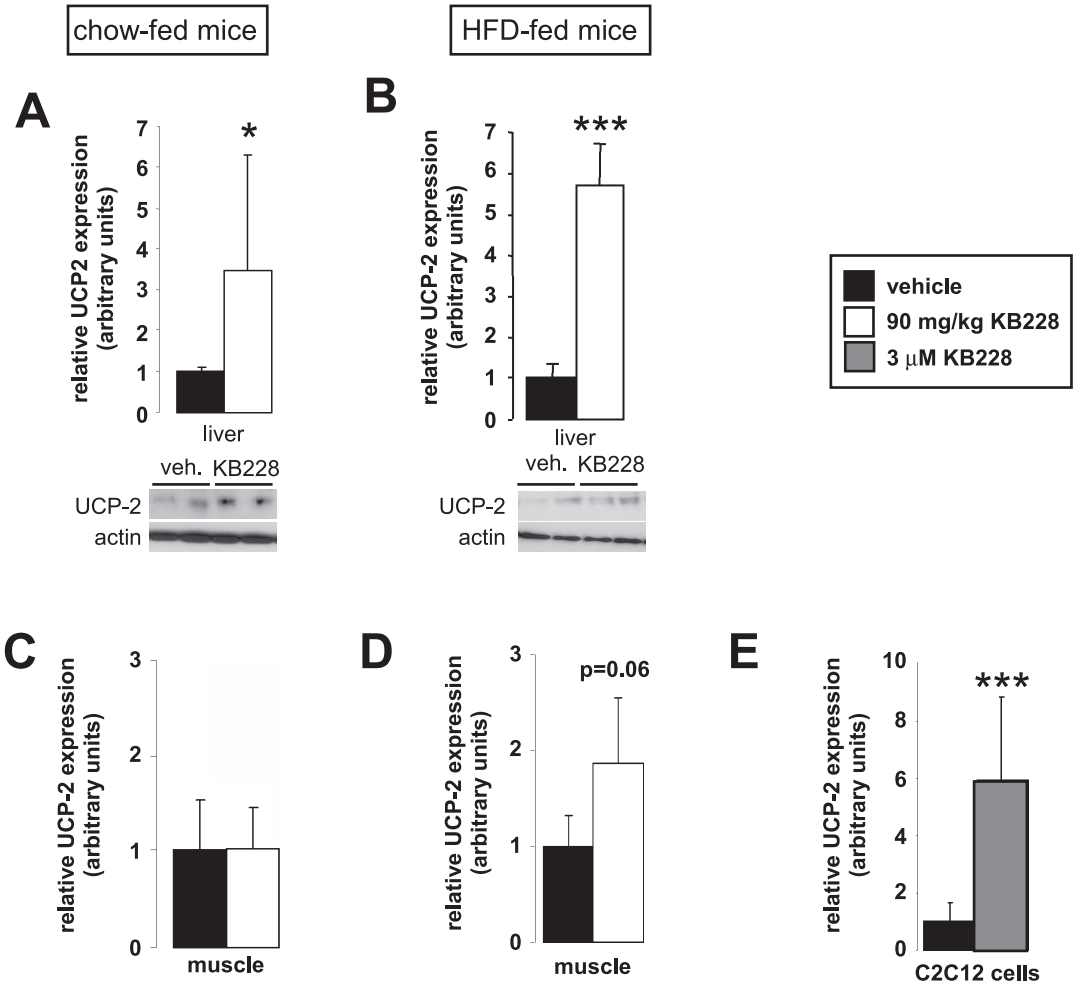

Figure 6. UCP2 induction by KB228. Chow-fed (n = 7/7, 6 months of age) and HFD-fed (n = 9/9, 6 months of age) C57/Bl6J male mice underwent vehicle or KB228 treatment. 2 hours post-treatment livers and gastrocnemius muscles were removed and homogenized. (A, B) In liver homogenates from chow-fed (A) or HFD-fed (B) mice UCP2 mRNA and protein levels were assayed in RT-qPCR reactions and Western blotting. (C, D) In skeletal muscle homogenates from chow-fed (C) or HFD-fed (D) mice UCP2 mRNA levels were measured in RT-qPCR reactions. (E) Differentiated C2C12 myoblasts were treated with 3 μM of KB228 for 8 hours then UCP2 expression was determined in RT-qPCR reactions. Error is given as SD on panel E. * and *** indicate statistically significant difference between vehicle and GPi-treated groups at $p<0.05$, or $p<0.001$, respectively.
doi:10.1371/journal.pone.0069420.g006

Statistical Analysis

Significance was determined using unpaired t-test for unequal sized samples where $p<0.05$ was considered as significant. Error bars represent SEM unless stated otherwise.

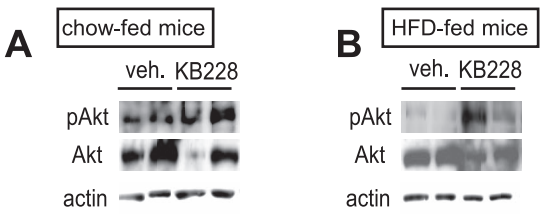

Figure 7. KB228 induced mTORC2 in mice. Chow-fed (n = 7/7, 6 months of age) and HFD-fed (n = 9/9, 6 months of age) C57/Bl6J male mice underwent vehicle or KB228 treatment (90 mg/kg). 2 hours post-treatment livers were removed and homogenized. From liver homogenates of chow-fed (A) and HFD-fed (B) mice Akt and phospho-Akt (^{473}Ser) levels were determined by Western blotting.
doi:10.1371/journal.pone.0069420.g007

Results

Preparation of N-(3,5-dimethyl-benzoyl)-N′-(β-D-glucopyranosyl)urea (KB228)

The glycogen phosphorylase inhibitor KB228 (*N*-(3,5-dimethyl-benzoyl)-*N*′-(β-D-glucopyranosyl)urea **4**) was prepared according to a previously published procedure [31] as shown in Fig. 1.: by treatment with oxalylchloride, 3,5-dimethyl-benzamide (**2**) was transformed into the corresponding acyl-isocyanate **3** which was reacted with β-D-glucopyranosylammonium carbamate (**1**) to yield the target compound **4**.

Biochemical and Physiological Characterization of KB228

KB228 displayed mixed type inhibition on purified rabbit muscle glycogen phosphorylase and the K_i of the inhibitor was calculated to be 0.93 ± 0.05 μM. Next, we set out to find an appropriate dose and administration of KB228 for *in vivo* studies. KB228 was administered to C57/Bl6J mice as a single i.p. injection in a 90 mg/kg dose (lower doses were ineffective – data not shown). KB228 treatment reduced blood glucose levels 30

minutes post treatment and the reduction was maintained for 6 hours (Fig. 2A) that coincided with an increment in hepatic glycogen content (Fig. 2B) without change in the expression of GP isoforms (Fig. 2C) suggesting that KB228 treatment was effective. We induced glucose intolerance and hampered insulin sensitivity (tested in ipGTT and ipITT, data not shown) by HFD feeding (3 months feeding). Significant increase in hepatic glycogen content confirmed the efficiency of GP inhibition (Fig. 2D). In that case we observed the induction of brain isotype GP (*pygb*), while other isoforms of GP did not change (Fig. 2E). The data validated the applicability of KB228 under normal and diabetic conditions in mice.

Effect of KB228 on Energy Balance

Given the long lasting effect of KB228, we performed indirect calorimetry experiments on C57/Bl6J mice that were on chow diet or HFD. Surprisingly, KB228 treatment enhanced oxygen consumption in chow-fed mice (Fig. 3A) suggesting an increased oxidative metabolism; and this result coincided with the higher respiratory quotient (RQ) found in chow-fed mice (Fig. 3B) indicative of higher glucose oxidation rates. In line with these data, KB228-treated mice displayed better glucose tolerance in ipGTT assays (Fig. 3C). Glucose uptake assays suggested that the main organ responsible for glucose excursion is the liver (Fig. 3D). KB228 treatment in HFD-fed animals had similar effects to chow-fed animals in terms of oxygen consumption and glucose tolerance (Fig. 3E–G). However, the improvement of their metabolic properties was less pronounced as compared to the chow-fed animals. There was only a slight increase in RQ on HFD instead of the significant enhancement on chow, furthermore ipGTT showed a weaker improvement (Fig. 3E–G), that was in line with the lower potency of KB228 to inhibit GP in hyperglycemic mice.

KB228 Treatment Induces UCP2 Expression and mTORC2 Activity

Our *in vivo* data suggested metabolic rearrangements in liver; therefore, we explored the *in vitro* metabolic effects of KB228 on HepG2 cells under normoglycemic (5.5 mM glucose in the medium) and hyperglycemic conditions (25 mM glucose in the medium). The expression of GP isoforms were unaltered both under normo and hyperglycemia (Fig. 4A, D) and KB228 treatment induced glycogen build-up (Fig. 4B, E) suggesting effective GP inhibition in both conditions. The administration of KB228 to HepG2 cells enhanced mitochondrial oxidation under normoglycemia (Fig. 4C). Treatments under hyperglycemia exerted negligible effects on mitochondrial oxidation (Fig. 4F).

In RT-qPCR reactions we have observed that the expression of uncoupling protein-2 (UCP2) was enhanced upon KB228 treatment in HepG2 cells. UCP2 mRNA and protein levels were induced by KB228 in a time-dependent manner (Fig. 4G–H). Induction of UCP2 expression and protein levels were not as pronounced in hyperglycemic conditions as in normoglycemia (Fig. 4G–H). UCP2 is a likely candidate to explain enhanced catabolism upon KB228 treatment.

We tested other potent GPi-s (TH, $K_i = 5.1$ μM [9], NV50, $K_i = 3$ μM [21] and NV76, $K_i = 0.47$ μM [14,22]) (Fig. 5A) on HepG2 cells cultured under normoglycemic conditions. These GPi-s efficiently inhibited GP as demonstrated by increases in cellular glycogen content (Fig. 5B). Furthermore, the treatment of cells with these GPi-s led to a ~2 fold induction of UCP2 expression (Fig. 5C) similarly to KB228. These data demonstrate that the induction of UCP2 is not limited to KB228 only but can be elicited by other inhibitors too. Furthermore, potency of the drugs to induce UCP-2 expression correlated with their respective K_i's.

Similarly to our findings in cellular models, KB228 induced UCP2 mRNA and protein content in the liver of chow and HFD-fed (diabetic) mice (Fig. 6A, B). However, the induction of UCP2 protein content was reduced in the diabetic mice when compared to the chow-fed control group. We assessed the expression of UCP2 in skeletal muscle samples. Although we did not detect changes in UCP2 expression in chow-fed mice (Fig. 6C), we have observed 2-fold induction in UCP2 mRNA levels in HFD-fed mice (Fig. 6D). Interestingly in C2C12 myoblasts a much larger, 6-fold enhancement of UCP2 expression was observed (Fig. 6E).

To assess further metabolic rearrangements triggered by KB228, we examined the activity of certain protein kinases involved in energy homeostasis, such as mTORC2 (assessed by detecting phosphorylation of Akt2 on ^{473}Ser) and Akt2 (assessed by detecting phosphorylation of GSK-3β on $^{9/21}$Ser) in mice. While we failed to detect changes in the phosphorylation of GSK-3β (data not shown), Akt2 phosphorylation on ^{473}Ser was enhanced upon KB228 treatment in control and diabetic mice despite lower Akt2 protein content (Fig. 7A, B) highlighting marked activation of mTORC2.

Discussion

In the present study we characterized the metabolic effects of a novel, potent GPi, KB228. As expected from previous studies with other GPi-s [8,9,15–18,32], KB228 reduced serum glucose levels and increased hepatic glycogen content under both normoglycemic and insulin resistant, hyperglycemic conditions. Surprisingly, glucose clearance was primarily attributed to the liver. Prior studies have suggested the involvement of skeletal muscle in GPi-induced glucose clearance [8], however upon KB228 treatment we did not detect increased glucose uptake in skeletal muscle, suggesting that KB228 action was rather restricted to the liver. However, it must be noted that we have observed the induction of UCP2 in murine gastrocnemius muscle and C2C12 cells despite the lack of enhanced glucose uptake. Our data point to the involvement of skeletal muscle in the glucose oxidation providing a likely explanation for the phenotype observed by Baker and co-workers [8].

The potency of KB228 to reduce glucose levels and to influence downstream molecular events was reduced under hyperglycemic conditions. GP effectors act through several binding sites on the enzyme [33,34]. KB228 displayed a mixed type inhibition suggesting the concurrent binding of the inhibitor to multiple sites, among them probably to the catalytic site. It is likely that the glucose moiety of KB228 competes with glucose for binding to the catalytic center of GP, therefore high glucose levels may reduce KB228 affinity to GP. Other glucose-based GPi-s were described to behave similarly under high glucose concentrations [9].

When we continued to uncover the molecular rearrangements and cellular effects induced by KB228 we found two parallel events that help the metabolic accommodation of cells to GPi treatment: induction of UCP2 expression and mTORC2 activity. UCP2 is a mitochondrial inner membrane protein that uncouples mitochondrial proton gradient from ATP production [35]. Higher level of uncoupling may induce the flux of the electron transport chain [36] therefore induction of UCP2 expression explains higher oxygen consumption. What could be the benefit from the induction of UCP2 expression? Excess glucose influx has been shown to produce hydroxyl radicals of mitochondrial origin due to the stalling of the mitochondrial electron transport chain [37]. UCP2 is capable of releasing that blockade therefore its induction

is considered to protect against oxidative stress [38,39]. It is presumable that UCP2 activation by KB228 treatment may have the same rationale, whereby UCP2 neutralize the excess glucose influx-induced mitochondrial free radical production analogously to the situation of enhanced hepatic fatty acid accumulation and catabolism [40,41]. Furthermore, it is possible that UCP2 expression might have contributed to the glucose lowering effect of KB228 through enhancing energy expenditure in liver. In fact, long term GPi application was reported to have adverse effects characterized by hepatic lipid and glycogen deposition [42]. UCP2 overexpression, however may have beneficial effects over these adverse effects that could be exploited to counteract hepatic lipid and glycogen accumulation upon long term GPi treatment.

mTOR, which was also found to be induced by KB228 treatment, is a conserved Ser/Thr protein kinase functioning as a master regulator of metabolism existing in two distinct complexes called complex 1 (mTORC1) and complex 2 (mTORC2) [43]. The defining component of mTORC2 is Rictor (rapamycin-insensitive companion of mTOR) that may serve to recruit substrates to mTORC2. Little is known to date on the upstream inputs and functions of mTORC2, however it seems that mTORC2 is insensitive to nutrient levels, but it is activated in response to insulin and growth factor receptor activation [44]. Yet two targets of mTORC2 have been identified, Akt2 and SGK [44]. ^{473}Ser phosphorylation of Akt2 seems to be an mTORC2 specific site. Phosphorylation of ^{473}Ser Akt2 leads to a restricted-type activation of Akt2, whereby Akt2 can phosphorylate only a limited set of its downstream targets (such as FOXO1 and FOXO3) in contrast to phosphorylation and activation by mTORC1 [45]. In liver, mTORC2 activation induces nutrient storage (glycogen and fatty acid synthesis) and glycolysis [46,47]. Therefore, mTORC2 activation may contribute to glycogen synthesis. Moreover, mTORC2 activity has been implicated in the hormonal rearrangement, termed hepatic satiety [47], a puzzling effect that could be investigated in relation to GP activity in the future.

The molecular events through which KB228 treatment leads to mTORC2 activation is unknown, but in any case, it is intriguing. That process can be termed retrograde signaling, as the inhibition of GP, an enzyme lying downstream of Akt2, in fact, leads to the activation of mTORC2 or alterations in insulin signaling, both lying upstream of Akt2. However, it cannot be excluded that simply glucose influx rearranges mTOR signaling, whereby cells sense glucose plenitude and turn towards storage that is glycogen build-up.

In summary, our data highlight that GP inhibition by KB228 treatment exerts more effects than a simple inhibition of catalytic activity. Our data show that glycogen metabolism interacts with mTORC2 and mitochondrial signaling. Recent research have shown that appropriate glycogen catabolism is a vital part of cellular glucose metabolism that is indispensable in sustaining cell cycle [48,49] or preventing cellular senescence [49]. Taken together with the data presented hereby strongly suggests that GP might be involved in a complex metabolic regulatory network that could be exploited in the management of diabetes, metabolic diseases or anti-Warburg strategies.

Acknowledgments

We acknowledge the technical help of Ms. Erzsébet Herbály and Ms. Ella Kovács. The authors highly appreciate the helpful discussions on the present manuscript with Dr. Péter Fülöp (Department of Internal Medicine, University of Debrecen).

Author Contributions

Conceived and designed the experiments: LS PG BP. Performed the experiments: LN TD AB MS CH JM. Analyzed the data: LN TD AB MS CH JM BK. Wrote the paper: LV LS PG PB. Synthesized KB228: BK LS.

References

1. Taniguchi CM, Emanuelli B, Kahn CR (2006) Critical nodes in signalling pathways: insights into insulin action. Nat Rev Mol Cell Biol 7: 85–96.
2. Stalmans W, Bollen M, Mvumbi L (1987) Control of glycogen synthesis in health and disease. Diabetes Metab Rev 3: 127–161.
3. Stalmans W, Bollen M, Toth B, Gergely P (1990) Short-term hormonal control of protein phosphatases involved in hepatic glycogen metabolism. Adv Enzyme Regul 30: 305–327.
4. Zhang T, Wang S, Lin Y, Xu W, Ye D, et al. (2012) Acetylation negatively regulates glycogen phosphorylase by recruiting protein phosphatase 1. Cell Metab 15: 75–87.
5. Aiston S, Hampson L, Gomez-Foix AM, Guinovart JJ, Agius L (2001) Hepatic glycogen synthesis is highly sensitive to phosphorylase activity: evidence from metabolic control analysis. J Biol Chem 276: 23858–23866.
6. Aiston S, Peak M, Agius L (2000) Impaired glycogen synthesis in hepatocytes from Zucker fatty fa/fa rats: the role of increased phosphorylase activity. Diabetologia 43: 589–597.
7. Agius L (2010) Physiological control of liver glycogen metabolism: lessons from novel glycogen phosphorylase inhibitors. Mini Rev Med Chem 10: 1175–1187.
8. Baker DJ, Greenhaff PL, MacInnes A, Timmons JA (2006) The experimental type 2 diabetes therapy glycogen phosphorylase inhibition can impair aerobic muscle function during prolonged contraction. Diabetes 55: 1855–1861.
9. Docsa T, Czifrak K, Huse C, Somsak L, Gergely P (2011) Effect of glucopyranosylidene-spiro-thiohydantoin on glycogen metabolism in liver tissues of streptozotocin-induced and obese diabetic rats. Mol Med Report 4: 477–481.
10. Newgard CB, Hwang PK, Fletterick RJ (1989) The family of glycogen phosphorylases: structure and function. Crit Rev Biochem Mol Biol 24: 69–99.
11. Agius L (2007) New hepatic targets for glycaemic control in diabetes. Best Pract Res Clin Endocrinol Metab 21: 587–605.
12. Bollen M, Keppens S, Stalmans W (1998) Specific features of glycogen metabolism in the liver. Biochem J 336 (Pt 1): 19–31.
13. Aiston S, Green A, Mukhtar M, Agius L (2004) Glucose 6-phosphate causes translocation of phosphorylase in hepatocytes and inactivates the enzyme synergistically with glucose. Biochem J 377: 195–204.
14. Somsak L, Czifrak K, Toth M, Bokor E, Chrysina ED, et al. (2008) New inhibitors of glycogen phosphorylase as potential antidiabetic agents. Curr Med Chem 15: 2933–2983.
15. Kelsall IR, Rosenzweig D, Cohen PT (2009) Disruption of the allosteric phosphorylase a regulation of the hepatic glycogen-targeted protein phosphatase 1 improves glucose tolerance in vivo. Cell Signal 21: 1123–1134.
16. Martin WH, Hoover DJ, Armento SJ, Stock IA, McPherson RK, et al. (1998) Discovery of a human liver glycogen phosphorylase inhibitor that lowers blood glucose in vivo. Proc Natl Acad Sci U S A 95: 1776–1781.
17. Furukawa S, Murakami K, Nishikawa M, Nakayama O, Hino M (2005) FR258900, a novel glycogen phosphorylase inhibitor isolated from Fungus No. 138354. II. Anti-hyperglycemic effects in diabetic animal models. J Antibiot (Tokyo) 58: 503–506.
18. Lerin C, Montell E, Nolasco T, Garcia-Rocha M, Guinovart JJ, et al. (2004) Regulation of glycogen metabolism in cultured human muscles by the glycogen phosphorylase inhibitor CP-91149. Biochem J 378: 1073–1077.
19. Varga G, Docsa T, Gergely P, Juhasz L, Somsak L (2012) Synthesis of tartaric acid analogues of FR258900 and their evaluation as glycogen phosphorylase inhibitors. Bioorg Med Chem Lett: doi: 10.1016/j.bmcl.2013.1001.1042.
20. Somsak L (2011) Glucose derived inhibitors of glycogen phosphorylase. Compt Rend Chimie 14: 211–223.
21. Nagy V, Felfoldi N, Konya B, Praly JP, Docsa T, et al. (2012) N-(4-Substituted-benzoyl)-N'-(beta-d-glucopyranosyl)ureas as inhibitors of glycogen phosphorylase: Synthesis and evaluation by kinetic, crystallographic, and molecular modelling methods. Bioorg Med Chem 20: 1801–1816.
22. Oikonomakos NG, Somsak L (2008) Advances in glycogen phosphorylase inhibitor design. Curr Opin Investig Drugs 9: 379–395.
23. Speziale AJ, Smith LR, Fedder J (1965) The Reaction of Oxalyl Chloride with Amides. IV. Synthesis of Acyl Isocyanates. J Org Chem 30: 4306–4307.
24. Braña MF, López Rodriguez ML (1981) Synthesis and reactivity of N-[α-acetoxy)-4-pyridylmethyl]-3,5-dimethylbenzamide. J Het Chem 18: 869–871.
25. Likhosherstov LM, Novikova OS, Shibaev VN (2002) New efficient synthesis of beta-glucosylamines of mono- and disaccharides with the use of ammonium carbamate. Dokl Chem 383: 89–92.
26. Osz E, Somsak L, Szilagyi L, Kovacs L, Docsa T, et al. (1999) Efficient inhibition of muscle and liver glycogen phosphorylases by a new glucopyranosylidene-spiro-thiohydantoin. Bioorg Med Chem Lett 9: 1385–1390.

27. Bai P, Canto C, Brunyanszki A, Huber A, Szanto M, et al. (2011) PARP-2 Regulates SIRT1 Expression and Whole-Body Energy Expenditure. Cell Metab 13: 450–460.
28. Bai P, Canto C, Oudart H, Brunyanszki A, Cen Y, et al. (2011) PARP-1 Inhibition Increases Mitochondrial Metabolism through SIRT1 Activation. Cell Metab 13: 461–468.
29. Szanto M, Rutkai I, Hegedus C, Czikora A, Rozsahegyi M, et al. (2011) Poly(ADP-ribose) polymerase-2 depletion reduces doxorubicin-induced damage through SIRT1 induction. Cardiovasc Res 92: 430–438.
30. Brunyanszki A, Hegedus C, Szanto M, Erdelyi K, Kovacs K, et al. (2010) Genetic Ablation of PARP-1 Protects Against Oxazolone-Induced Contact Hypersensitivity by Modulating Oxidative Stress. J Invest Dermatol 130: 2629–2637.
31. Somsák L, Felföldi N, Kónya B, Hüse C, Telepó K, et al. (2008) Assessment of synthetic methods for the preparation of *N*-β-D-glucopyranosyl-*N*'-substituted ureas, -thioureas and related compounds. Carbohydr Res 343: 2083–2093.
32. Baker DJ, Timmons JA, Greenhaff PL (2005) Glycogen phosphorylase inhibition in type 2 diabetes therapy: a systematic evaluation of metabolic and functional effects in rat skeletal muscle. Diabetes 54: 2453–2459.
33. Chrysina ED (2010) The prototype of glycogen phosphorylase. Mini Rev Med Chem 10: 1093–1101.
34. Chrysina ED, Kosmopoulou MN, Tiraidis C, Kardakaris R, Bischler N, et al. (2005) Kinetic and crystallographic studies on 2-(beta-D-glucopyranosyl)-5-methyl-1, 3, 4-oxadiazole, -benzothiazole, and -benzimidazole, inhibitors of muscle glycogen phosphorylase b. Evidence for a new binding site. Protein Sci 14: 873–888.
35. Baffy G, Zhang CY, Glickman JN, Lowell BB (2002) Obesity-related fatty liver is unchanged in mice deficient for mitochondrial uncoupling protein 2. Hepatology 35: 753–761.
36. Pesta D, Gnaiger E (2012) High-resolution respirometry: OXPHOS protocols for human cells and permeabilized fibers from small biopsies of human muscle. Methods Mol Biol 810: 25–58.
37. Nishikawa T, Edelstein D, Du XL, Yamagishi S, Matsumura T, et al. (2000) Normalizing mitochondrial superoxide production blocks three pathways of hyperglycaemic damage. Nature 404: 787–790.
38. Arsenijevic D, Onuma H, Pecqueur C, Raimbault S, Manning BS, et al. (2000) Disruption of the uncoupling protein-2 gene in mice reveals a role in immunity and reactive oxygen species production. Nat Genet 26: 435–439.
39. Adam-Vizi V, Chinopoulos C (2006) Bioenergetics and the formation of mitochondrial reactive oxygen species. Trends Pharmacol Sci 27: 639–645.
40. Horimoto M, Fulop P, Derdak Z, Wands JR, Baffy G (2004) Uncoupling protein-2 deficiency promotes oxidant stress and delays liver regeneration in mice. Hepatology 39: 386–392.
41. Fulop P, Derdak Z, Sheets A, Sabo E, Berthiaume EP, et al. (2006) Lack of UCP2 reduces Fas-mediated liver injury in ob/ob mice and reveals importance of cell-specific UCP2 expression. Hepatology 44: 592–601.
42. Floettmann E, Gregory L, Teague J, Myatt J, Hammond C, et al. (2010) Prolonged inhibition of glycogen phosphorylase in livers of Zucker Diabetic Fatty rats models human glycogen storage diseases. Toxicol Pathol 38: 393–401.
43. Guertin DA, Sabatini DM (2007) Defining the role of mTOR in cancer. Cancer Cell 12: 9–22.
44. Laplante M, Sabatini DM (2012) mTOR signaling in growth control and disease. Cell 149: 274–293.
45. Guertin DA, Stevens DM, Thoreen CC, Burds AA, Kalaany NY, et al. (2006) Ablation in mice of the mTORC components raptor, rictor, or mLST8 reveals that mTORC2 is required for signaling to Akt-FOXO and PKCalpha, but not S6K1. Dev Cell 11: 859–871.
46. Zoncu R, Efeyan A, Sabatini DM (2011) mTOR: from growth signal integration to cancer, diabetes and ageing. Nat Rev Mol Cell Biol 12: 21–35.
47. Hagiwara A, Cornu M, Cybulski N, Polak P, Betz C, et al. (2012) Hepatic mTORC2 activates glycolysis and lipogenesis through Akt, glucokinase, and SREBP1c. Cell Metab 15: 725–738.
48. Colombo SL, Palacios-Callender M, Frakich N, Carcamo S, Kovacs I, et al. (2011) Molecular basis for the differential use of glucose and glutamine in cell proliferation as revealed by synchronized HeLa cells. Proc Natl Acad Sci U S A 108: 21069–21074.
49. Favaro E, Bensaad K, Chong MG, Tennant DA, Ferguson DJ, et al. (2012) Glucose Utilization via Glycogen Phosphorylase Sustains Proliferation and Prevents Premature Senescence in Cancer Cells. Cell Metab 16: 751–764.